

# ZERO ORDER AND CONJUGATE IMAGES ELIMINATION FOR DIGITAL HOLOGRAMS

HANAN HALAQ<sup>1</sup>, YOSHITATE TAKAKURA<sup>2</sup>, and DALIBOR VUKICEVIC<sup>2</sup>

<sup>1</sup>LISAC Laboratory, Faculty of Sciences Dhar El Mehraz, University (USMBA), Department of physics, Fez, Morocco

<sup>2</sup>Engineering Science, Computer Science and Imaging Laboratory (ICube), Télécom Physique Strasbourg, University of Strasbourg, Illkirch-Graffenstaden, France

E-mail: <sup>1</sup>hanan.halaq@usmba.ac.ma, <sup>2</sup>y.takakura@unistra.fr, Dalibor Vukicevic deceased on September 1<sup>st</sup> 2016

## ABSTRACT

The zero order and the twin image severely affect the quality of reconstructions in digital holography, as a result of limited resolution and dynamic range of camera sensors. Several techniques have been proposed to minimize or to eliminate those elements. Some are purely numerical; others require experimental interventions. Amongst them are: subtraction digital holography that consists of subtracting a randomly modified recording from the original one, HRO and phase shifting methods that use controlled images for subtraction. We have investigated these methods theoretically and experimentally for both off-axis Fourier and Fresnel holography. Their performance has been assessed with a sample that is a vibrating membrane in the former case, and a stick-shaped transmission diffuser in the latter case. Experimental evidence indicates that if they are efficient for zero-order elimination on off-axis Fourier holograms, a simple digital procedure applied to a single Fresnel recording, and that combines mean value subtraction and spatial filtering in the frequency space permits remove the zero order and the twin image simultaneously.

**Keywords:** *Quasi-Fourier Off-axis Digital Holography; Fresnel Digital Holography; Filtering Technique; Zero order and Conjugate Image.*

## 1. INTRODUCTION

In the original Gabor in-line configuration, holography suffers from limitations which restrict its applicability [1]. In such a holographic setup, the axis which points at the direction of propagation of the object wave, and the one of the reference wave are colinear. As a consequence, the hologram reconstruction is composed of the actual object wave, the un-diffracted reconstruction wave (the zero-order image, also called the dc term) and the so-called twin image (or virtual image) wave. The problem is not the presence of the twin image per se, but rather its inseparability from the original image [2]. A number of methods have been proposed for eliminating or reducing the twin-image problem, the most successful being the one achieved by Leith and Upatnieks. The off-axis geometry introduced by Leith and Upatnieks separated the three images which made holography and holographic interferometry feasible [3]. This type of hologram is called the Leith-Upatnieks hologram, also known as

the offset-reference hologram. The major difference between this type of hologram and the Gabor hologram is that, rather than using the light directly transmitted by the object as a reference wave, a separate different reference is introduced. It is introduced with an offset angle, rather than along the object-film axis. The fact is that, if the spatial bandwidth of the object wave is sufficiently small compared to the carrier of the reference wave, such a component will remain sufficiently close to the optical axis so as to be spatially separated from the images of interest. When such condition on the bandwidth is not satisfied, overlapping of diffraction orders (-1, 0, +1) occurs.

In the conventional off-axis holography, recording and reconstruction are achieved optically on fine grain photo emulsions [4]. As for digital holography, recording is achieved with CCD cameras (or CMOS) and numerically reconstructed by means of a computer software. Digital holograms are obtained by Fourier transforming the recorded data and by

observing their amplitude. Due to the sampling process, this is necessarily a discrete operation. In practice a Fast Fourier Transform (FFT) is used, which allows fast computing of discrete Fourier transforms (DFT) of large image arrays. In opposition to the analog case, effective methods have been proposed to eliminate the dc term and the twin image in digital holography: some are purely numerical [5]; others require experimental intervention [6-11]. These latter methods will be referred to as hybrid methods. As for the elimination of the zero-order disturbance, Kreis and Jüptner [5] proposed a purely numerical method which consists of subtracting the average intensity from each stored hologram. This is actually a high-pass filtering with a cutoff frequency equal to the smallest non-zero frequency. For hybrid holographic microscopy, T.-C. Poon, K.B. Doh, B.W. Schilling, M.H. Wu, K. Shinoda and Y. Suzuki [6] proposed an approach based on scanning a three-dimensional object by a time-dependent Fresnel zone-lens plate. Such a technique results in object reconstructions without the zero-order disturbance but is a slow process because of the scanning operation. Y. Takaki, H. Kawai and H. Ohzu [7] compared methods for eliminating the zero-order image and the conjugated image by using two shutters and a liquid-crystal phase modulator to change recording parameters. These methods are: 1. to eliminate the zero order, three images are captured from which the images of the reference only and of the object only are subtracted from the interference pattern, 2. to eliminate the zero order, two interference patterns with different phase shifts are captured and subtracted. 3. to eliminate the zero-order image and the conjugate image four images are captured. The first one is the intensity image of the object beam. The second image is the intensity of the reference beam. The third image is the interference pattern between the reference beam and the object beam. And the last image is the interference pattern with phase shift  $\alpha$  introduced between the reference beam and the object beam so that through a simple computing process, only the real image is obtained, 4. to eliminate the zero-order image and the conjugate image, three images are captured with respective phase difference of 0,  $\theta_1$  and  $\theta_2$  between the reference beam and the object beam so as to obtain the real image only. Theoretical validation will be given in this paper. M.L. Rodriguez, J.A. Rayas, R.R Cordero, A.M Garcia, A.M Gonzalez, A.T. Oufiñones, P. Contreras and O.M Cázares [8] applied 0 and  $\pi$  phase shift of the reference beam to suppress the twin-image and the zero-order

diffracted wave in the frequency domain by processing the recorded holograms. I. Yamaguchi and T. Zhang [9] proposed a solution which consists of multiple recordings with phase shifting. It requires four holograms recorded with phase shifts of 0,  $\pi/2$ ,  $\pi$  and  $3\pi/2$  to remove the undesired terms from a digital hologram and, without sacrificing any active area of a CCD. The drawback is that phase shifting must be achieved on a vibration-free optical table. This means that the method can only be used in the laboratory: it does not apply to targets moving during the recording procedure. N. Yoshikawa, S. Namiki and A. Uoya [10] proposed a three-step generalized phase-shifting method to remove zero-order terms by mutual subtraction of the phase-shifted holograms. N. Demoli, J. Mestrovic and I. Sovic [11] developed a method by subtracting two recordings which contain different stochastic speckled patterns and by reconstructing with a Fourier transform on the result. An iterative approach for twin image elimination has been presented by L. Onural and P.D. Scott [12] and, L. Onural and M.T. Ozgen [13].

G. Pedrini, P.Froning, H. Fessler and H.J. Tiziani [14] showed how the dc term and portion of the twin image can be eliminated with in-line digital holographic interferometry by applying a bandpass filter in the frequency domain. G.-L. Chen, C.-Y. Lin, M.-K.Kuo, and C.-C. Chang [15] developed an approach based on numerical operations to suppress zero-order images. It needs only one digital hologram but the intensity ratio of the object-to-reference waves must be kept under control during the recording procedure. It is simple, effective and consists of subtracting from the digital hologram the intensities of the object and reference waves generated numerically. They [16] also proposed an approach to suppress both the zero-order and the real images, by using an off-axis Fresnel digital hologram, which avoids any additional phase-retrieval elements in the experimental setup. It consists of multiplying the hologram and the reference, and of convoluting the result with a chirp function. N. Pavillon, C.S. Seelamantula, J. Kuhn, M. Unser, and C. Depeursinge [17] reported a robust purely numerical method based on nonlinear filtering to eliminate the zero-order term with application to off-axis digital holographic microscopy. Also, an iterative procedure for suppressing the zero-order without any a priori knowledge about the object has been released by the same research group [18]. Z. Ma *et al* [19] proposed a novel numerical iterative approach for effectively eliminating the zero-order term and to improve the

signal-to-noise ratio of the reconstructed image for off-axis digital holography.

Z. Dong, H. Wang and X. Wang [20] present an automatic filtering method. The filtered zone is a circle in the Fourier domain. With such a filtering method, the desired spectra can be filtered out automatically and non-iteratively. The method has been tested and validated on several samples. Compared to the iterative filtering method, it requires only 2% of its processing time and provides reconstructed images with high similarity.

H. Wang, M. Lyu, and G. Situ [21] reported eHoloNet, a learning-based one-step end-to-end approach for in-line holographic reconstruction. By using eHoloNet, one can directly reconstruct the object wavefront from a single-shot in-line hologram, with the removal of the unwanted zero-order and twin image terms. Z. Li, L. Li, Y. Qin, G. Li, D. Wang and X. Zhou [22] proposed a double-distance reconstruction algorithm which iteratively, recovers phase information between the two recording planes to suppress the twin-image and zero-order artifacts. The reconstructed results demonstrate the algorithm's effectiveness and it is the first time in THz digital holography that the wavefront of both object and illuminating background are reconstructed simultaneously.

Here, we expose four methods to eliminate the zero-order image and two to eliminate the zero-order image and the conjugate image. They are representative of digital holography. The paper is organized as follow: the first section deals with theoretical proofs of zero order and conjugate images elimination. Subtraction digital holography, HRO (Hologram, Reference, Object), phase shifting subtraction holography, mean value subtraction and digital low pass filter are reviewed. The second section illustrates the performance of each method with experimental holograms. Finally, the paper terminates with some concluding remarks.

## 2. THEORETICAL ANALYSES

### 2.1 Preliminary Calculations: Quasi-Fourier Off-axis Configuration

The considered configuration is a quasi-Fourier off-axis setup shown in Fig. 1. The point-source that generates spherical waves is located in the plane  $P_1$  of the object. A hologram recorded under these conditions can be assimilated to a Fourier hologram [9,10] because the spherical phase factor that appears in the Fresnel transform is eliminated by the spherical reference wave which

has the same curvature. As a consequence, the interference pattern is composed of sinusoidal fringes with a spatial frequency vector that is object-dependent.

Such fringes are recorded by a CCD sensor positioned in the hologram plane  $P_2$  and the object is reconstructed with a computer software.

With the point source located at position  $(x_0, y_0)$  on the same plane  $P_1$  as the object  $o_1(x_1, y_1)$ , the amplitude distribution  $u_1(x_1, y_1)$  of the total field may be written as in (1) [4]:

$$u_1(x_1, y_1) = R_0 \delta(x_1 - x_0, y_1 - y_0) + o_1(x_1, y_1) \quad (1)$$

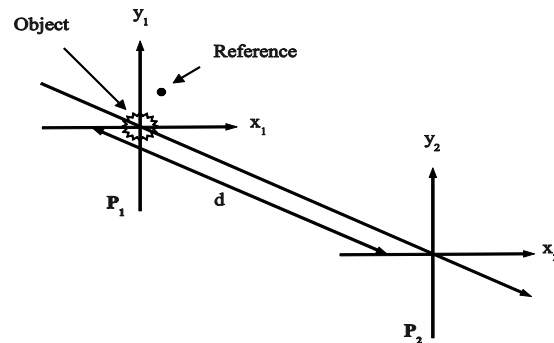


Figure 1: Quasi-Fourier Off-axis Configuration.

where  $R_0$  is the amplitude of the point source. The field  $u_2(x_2, y_2)$  on the CCD plane  $P_2$  can be calculated using the Fresnel diffraction formula [1]. It is given in (2):

$$u_2(x_2, y_2) = C \times E(x_2, y_2) \times [E(x_0, y_0) \exp(-2i\pi(x_0 f_x + y_0 f_y)) R_0 + \text{FT}\{E(x_1, y_1) o_1(x_1, y_1)\}] \quad (2)$$

where  $C$  is the complex constant  $(1/(i\lambda)) \exp(2i\pi d/\lambda)$ ,  $f_x = x_2/(\lambda d)$ ,  $f_y = y_2/(\lambda d)$  the spatial frequencies along  $x_2$  and  $y_2$  respectively, and  $E(x_n, y_n)$  is defined as the exponential  $\exp(i(\pi/(\lambda d))(x_n^2 + y_n^2))$  for  $n = 0, 1, 2$ . Finally, the symbol FT denotes the Fourier transform operator.

The second term in (2) is the object wavefront on the CCD plane. For convenience, it will be rewritten as:

$$\text{FT}\{E(x_1, y_1) o_1(x_1, y_1)\} = |o(x_2, y_2)| \exp(i\theta(x_2, y_2)), \text{ so that the intensity captured by the sensor is proportional to } I(x_2, y_2) \text{ as in (3):}$$

$$I(x_2, y_2) = R_0^2 + |o(x_2, y_2)|^2 + 2R_0 |o(x_2, y_2)| \cos(\theta_c(x_2, y_2)) \quad (3)$$

with  $\theta_c(x_2, y_2) = \theta(x_2, y_2) + (2\pi/(\lambda d)) [x_0(x_2 - x_0/2) + y_0(y_2 - y_0/2)]$ . This is the usual expression for interferences. It is more practical to express (3) in terms of (4):

$$I(x_2, y_2) = R_0^2 + |o(x_2, y_2)|^2 + R_0[J(x_2, y_2) + J^*(x_2, y_2)] \quad (4)$$

with  $J(x_2, y_2) = E^*(x_0, y_0) \exp(2i\pi(x_0 f_x + y_0 f_y)) o(x_2, y_2)$ , where the symbol \* designates the complex conjugate. Recalling that  $o(x_2, y_2)$  is the FT of  $E(x_1, y_1) o_1(x_1, y_1)$  and that successive applications of FT permit to retrieve the original function[17], ones gets the result of (5) as an FT is applied to the distribution  $I(x_2, y_2)$ :

$$FT\{I(x_2, y_2)\} = R_0^2 \delta(x_1, y_1) + \rho(x_1, y_1) + R_0[V(x_1, y_1) + V^*(-x_1, -y_1)] \quad (5)$$

where  $V(x_1, y_1) = E^*(x_0, y_0) E(-x_1 + x_0, -y_1 + y_0) o_1(-x_1 + x_0, -y_1 + y_0)$ ;  $\delta(x_1, y_1)$  is the Dirac impulse located at position  $(0, 0)$  and  $\rho(x_1, y_1)$  is the autocorrelation of  $E(x_1, y_1) o_1(x_1, y_1)$  according to the theorem of Wiener-Kinchin.

The physical interpretation of (5) is that the Fourier transform of the interferogram  $I(x_2, y_2)$  which results from a quasi-Fourier off-axis configuration may have three components. The first one is the undesired zero-order image located around position  $(0, 0)$ . It is constituted of a point-source which is the image of the reference, and the autocorrelation of a distribution that is closely related to the object. The two other components are the useful images to be retrieved; they represent the object shifted to position  $(x_0, y_0)$  and  $(-x_0, -y_0)$  respectively. The issue in digital holography is that for usual configurations with a given object, the shift  $\sqrt{x_0^2 + y_0^2}$  may not be large enough to spatially separate the components identified from (5).

## 2.2 Preliminary Calculations: the Case of Fresnel Holography

In the case of the more general Fresnel holography, the object is illuminated with a plane wave. The reference is also a plane wave with real amplitude  $R$ . Both object and reference are located in the same plane  $P_1$ . The light scattered from the object propagates towards the hologram plane  $P_2$  where it combines with the reference wave, and the resulting intensity pattern is recorded by a camera. A hologram obtained under these conditions is referred to as a Fresnel hologram because of the presence of a spherical phase factor that will be exposed in the following.

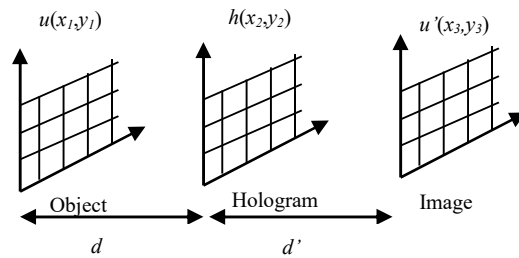


Figure 2: Fresnel Off-axis Configuration.

The geometry for the Fresnel configuration is shown in Fig. 2 where  $(x_1, y_1)$ ,  $(x_2, y_2)$  and  $(x_3, y_3)$  denote the coordinates in the object plane, the recording plane and the reconstruction plane respectively. The interference of the wave that has the complex amplitude:

$$O(x_2, y_2) = A_o(x_2, y_2) \exp[i\phi_o(x_2, y_2)]$$

that carries the object information, and the reference wave  $R(x_2, y_2) = R = R^*$ , results in four superimposed terms in the hologram plane  $(x_2, y_2)$ :

$$H(x_2, y_2) = (R(x_2, y_2) + O(x_2, y_2)) \cdot (R(x_2, y_2) + O(x_2, y_2))^* \quad (6)$$

$$= RR^* + OO^* + OR^* + O^*R$$

where the asterisks denote the complex conjugates. The first and the second terms in (6) are the intensities of the reference and object waves. They form the zero order. The remaining two terms represent the +1 and -1 orders that encode the information to be retrieved. As a matter of fact, the zero order is much more brighter than the first-order terms, so that visualization of the latter requires contrast enhancement.

The amplitude distribution  $u'(x_3, y_3)$  of the total field at the image plane may be written as in (7):

$$u'(x_3, y_3) = \frac{1}{i\lambda d'} \exp\left(i \frac{2\pi}{\lambda} d'\right) \int_{-\infty}^{+\infty} \int_{-\infty}^{+\infty} H(x_2, y_2) R(x_2, y_2) \exp\left[i \frac{\pi}{\lambda d} ((x_2 - x_3)^2 + (y_2 - y_3)^2)\right] dx_2 dy_2 \quad (7)$$

Developing the quadratic term in the exponential leads to expression (8):

$$u'(x_3, y_3) = \frac{1}{i\lambda d'} \exp\left(i \frac{2\pi}{\lambda} d'\right) \exp\left[i \frac{\pi}{\lambda d'} (x_3^2 + y_3^2)\right] \left[ \int_{-\infty}^{+\infty} \int_{-\infty}^{+\infty} h(x_2, y_2) R(x_2, y_2) \exp\left[i \frac{\pi}{\lambda d'} (x_2^2 + y_2^2)\right] \exp\left[-i \frac{2\pi}{\lambda d'} (x_3 x_2 + y_3 y_2)\right] dx_2 dy_2 \right] \quad (8)$$

which is the so-called Fresnel approximation or Fresnel transform, in mathematical similarity to the Fourier transform. Posing  $f_x = \frac{x_3}{\lambda d'}$ ,  $f_y = \frac{y_3}{\lambda d'}$ , which define the spatial frequencies along  $x_3$  and  $y_3$  respectively, equation (9) is obtained:

$$u'(x_3, y_3) = \frac{1}{i\lambda d'} \exp\left(i\frac{2\pi}{\lambda}d'\right) \cdot \exp[i\pi\lambda d'(f_x^2 + f_y^2)] \cdot \left[ \int_{-\infty}^{+\infty} \int_{-\infty}^{+\infty} H(x_2, y_2) R(x_2, y_2) \cdot \exp\left[i\frac{\pi}{\lambda d'}(x_2^2 + y_2^2)\right] \cdot \exp[-i2\pi(x_2 f_x + y_2 f_y)] dx_2 dy_2 \right] \quad (9)$$

It is worth noting that the Fresnel approximation is the Fourier transform of hologram  $H(x_2, y_2)$  multiplied with the reference wave  $R(x_2, y_2)$  and the quadratic phase function:  $\exp\left[i\frac{\pi}{\lambda d'}(x_2^2 + y_2^2)\right]$ .

$$u'(f_x, f_y) = \frac{1}{i\lambda d'} \exp\left(i\frac{2\pi}{\lambda}d'\right) \exp[i\pi\lambda d'(f_x^2 + f_y^2)] \cdot \text{FT}\left\{H(x_2, y_2) \exp\left[i\frac{\pi}{\lambda d'}(x_2^2 + y_2^2)\right]\right\} \quad (10)$$

We will now expose some relevant methods used to remove the zero-order component in digitally reconstructed holograms.

### 2.3 Subtraction Digital Holography[11]

In subtraction digital holography, the zero-order image is eliminated by capturing two interferograms in different uncontrolled conditions and subtracted. Object reconstruction is achieved by applying a DFT on the subtracted image. We shall expose and discuss the justification that has been given [11].

If the recording setup is subject to random phenomena that would slightly modify the interference patterns, the two recorded images would differ from each other by small amount of displacements. Consequently, the second recording  $I_{shift}(x_2, y_2)$  can be written in terms of the first one  $I(x_2, y_2)$  as in (11):

$$I_{shift}(x_2, y_2) = I(x_2 + \Delta x_2, y_2 + \Delta y_2) \quad (11)$$

where  $\Delta x_2$  and  $\Delta y_2$  designate local displacements around  $x_2$  and  $y_2$ . Under such assumptions,  $I_{shift}(x_2, y_2)$  can be expressed in terms of a Taylor expansion so that the difference  $\Delta I(x_2, y_2)$  between  $I_{shift}(x_2, y_2)$  and  $I(x_2, y_2)$  can be written as in (12):

$$\Delta I(x_2, y_2) = \Delta x_2 \frac{\partial I}{\partial x}(x_2, y_2) + \Delta y_2 \frac{\partial I}{\partial y}(x_2, y_2) \quad (12)$$

In practice, the interferogram  $I(x_2, y_2)$  may be regularly sampled so that the recorded interferogram

reads  $I_{k,l} = I(kh_x, lh_y)$  where  $k$  and  $l$  are integers,  $h_x$  and  $h_y$  are the sampling steps along  $x_2$  and  $y_2$  respectively. Consequently, the corresponding subtracted digital hologram  $\Delta I_{k,l}$  would be approximated by the expression of (13):

$$\Delta I_{k,l} = u_{k,l} \frac{I_{k+1,l} - I_{k-1,l}}{2h_x}(x_2, y_2) + v_{k,l} \frac{I_{k,l+1} - I_{k,l-1}}{2h_y} \quad (13)$$

where  $u_{k,l}$  and  $v_{k,l}$  represent shifts along  $x_2$  and  $y_2$  directions at position  $(k, l)$ . At this point, it is useful to introduce the kernel  $K_{k,l}$  as in (14):

$$K_{k,l} = \begin{bmatrix} 0 & -v_{k,l}/(2h_y) & 0 \\ -u_{k,l}/(2h_x) & 0 & u_{k,l}/(2h_x) \\ 0 & v_{k,l}/(2h_y) & 0 \end{bmatrix} \quad (14)$$

where  $u_{k,l}$  and  $v_{k,l}$  are index independent,  $K_{k,l}$  can be assimilated to the kernel of an ideal high-pass filter along  $x_2$  and  $y_2$  [18]. In such a case, Equation (8) can be identified as a 2D discrete convolution which defines  $\Delta I_{k,l}$  as a high-pass filtered image of  $I_{k,l}$ . As a consequence, since the original object is reconstructed from  $\Delta I_{k,l}$  by applying a DFT, low frequencies that build the zero-order image are removed and high frequencies which correspond to high diffraction orders are reconstructed from the DFT. This means that the zero-order elimination in subtraction digital holography could be assimilated to a digital high-pass filtering process.

### 2.4 Digital High-pass Filtering

In order to verify that the zero-order elimination in subtraction digital holography could be assimilated to a digital high-pass filtering process, a merit function  $L_2$  such as the one in (15) is introduced:

$$L_2 = \sum_{k,l} [\Delta I_{k,l} - a(I_{k+1,l} - I_{k-1,l}) - b(I_{k,l+1} - I_{k,l-1})]^2 \quad (15)$$

with  $a = u_{k,l}/(2h_x)$ ,  $b = v_{k,l}/(2h_y)$ , and minimized. The DFT of the ideally filtered image  $(\Delta I_{k,l})_{ideal} = a(I_{k+1,l} - I_{k-1,l}) + b(I_{k,l+1} - I_{k,l-1})$  is then calculated, compared to the DFT of  $I_{k,l}$  and to the DFT of the experimental subtracted digital hologram  $\Delta I_{k,l}$ . The results of a case study are given in Fig. 3 where  $a = -0.402$  and  $b = -0.110$ .

There is evidence to indicate that the zero-order elimination in subtraction digital holography cannot be solely explained by the high-pass filtering process that has been exposed. For example, the point-source and the autocorrelation of the object which constitute the zero-order image in the DFT of the interferogram (Image 3a) have been completely removed from the

subtracted digital hologram (Image 3c) while they are only partially altered in the image reconstructed from the interferogram filtered digitally (Image 3b). Besides, in the latter image, the reconstructed object has also been affected by the digital high-pass filter, as proved by the image difference (Image 3d). From such analyses, we believe that the justification of the zero-order elimination based on the Taylor expansion of (12) is unsatisfying; it should rely on changes that might affect the phase difference in-between recordings. This is the object of the following sections.

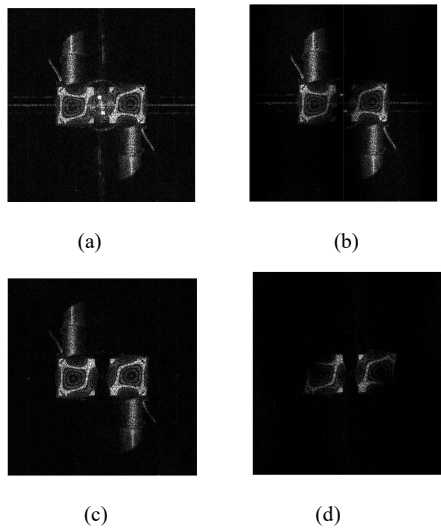


Figure 3: Zero-order Elimination: a) DFT of an Interferogram, b) Digital Highpass Filter, c) Subtraction Digital Holography, d) Difference a-b.

### 2.5 HRO Method [7]

This method is based on using two shutters and requires the capture of three images. The first one is the intensity image of the object beam. It corresponds to  $I_o = |o(x_2, y_2)|^2$  and is recorded by switching off the reference wave [7]. The second image is the intensity of the reference beam  $I_R = R_0^2$ . It is obtained by switching off the object wave. Finally, the last image is the interference pattern  $I(x_2, y_2)$  between the reference beam and the object beam. We shall now assess results that are also valid for phase shifting subtraction holography.

The intensity difference  $\Delta I(x_2, y_2)$  here is equal to the difference between the recorded interference pattern  $I(x_2, y_2)$ , the recorded reference intensity  $I_R$  and the recorded object intensity  $I_o$ . It is given by (16):

$$\Delta I(x_2, y_2) = I(x_2, y_2) - R_0^2 - |o(x_2, y_2)|^2 = 2R_0 |o(x_2, y_2)| \cos(\theta_c(x_2, y_2)) \quad (16)$$

Using previous calculations,  $\Delta I(x_2, y_2)$  can be rewritten as in (17):

$$\Delta I(x_2, y_2) = R_0 [J(x_2, y_2) + J^*(x_2, y_2)] \quad (17)$$

with  $J(x_2, y_2) = E^*(x_0, y_0) \exp(2i\pi(x_0 f_x + y_0 f_y)) o(x_2, y_2)$ , where the symbol \* designates the complex conjugate. In practice, like in subtraction digital holography, reconstruction is achieved by applying a DFT to the sampled intensity difference  $\Delta I(kh_x, lh_y)$ . The reconstructed digital hologram  $U(p, q)$  is then given by (18):

$$U(p, q) = R_0 [V(p, q) + V^*(-p, -q)] \quad (18)$$

$$V(p, q) = E^*(x_0, y_0) \sum_{k, l} o(kh_x, lh_y) \exp\left(2i\pi\left(k\left(-\frac{p}{N_x} + \frac{x_0 h_x}{\lambda d}\right) + l\left(-\frac{q}{N_y} + \frac{y_0 h_y}{\lambda d}\right)\right)\right) \quad (19)$$

where  $p, q$  are integers and  $N_x, N_y$  represent the amount of samples along  $x_2, y_2$ . The second term in (14) is the DFT of  $o(kh_x, lh_y)$  with indexes shifted to  $p_0 = x_0 h_x N_x / (\lambda d)$  and  $q_0 = y_0 h_y N_y / (\lambda d)$  respectively. Since  $o(x_2, y_2)$  is the Fourier transform of  $E(x_1, y_1) o_1(x_1, y_1)$  and from the fact that successive applications of FT permit to retrieve the original function, Equation (19) can be rewritten as in (20):

$$V(p, q) = E^*(x_0, y_0) \times E\left(-\frac{p}{N_x} \cdot \frac{\lambda d}{h_x} + x_0, -\frac{q}{N_y} \cdot \frac{\lambda d}{h_y} + y_0\right) \times O_1\left(-\frac{p}{N_x} \cdot \frac{\lambda d}{h_x} + x_0, -\frac{q}{N_y} \cdot \frac{\lambda d}{h_y} + y_0\right) \quad (20)$$

The term  $O_1$  is extracted from the DFT of the FT of  $E(x_1, y_1) o_1(x_1, y_1)$ . Because DFT and FT do not have exactly the same mathematical properties,  $O_1$  cannot be equal to  $o_1$ . However, it is reasonable to consider that  $O_1$  is an estimate of  $o_1$  that gives correct geometrical descriptions such as shapes. As a consequence,  $V(p, q)$  represents an estimate of the original object shifted to position  $(p_0, q_0)$  while  $V^*(-p, -q)$  is at position  $(-p_0, -q_0)$ : there is no zero order in the hologram  $U(p, q)$  reconstructed with the HRO method. It is worth noting that if the size of the object to be recorded is known, Equation (21) permits to access to conditions under which the orders  $V(p, q)$  and  $V^*(-p, -q)$  do not overlap. This is important to obtain spatially resolved digital holograms.

The drawback of the HRO method is that it needs the capture of three images in rigorously the same conditions: the interference pattern, the reference intensity and the object intensity. It is very unlikely to work in a fluctuating environment where the previously exposed subtraction digital holography can be effective. In the next section, we shall see that the number of images to be captured can be reduced to two, provided that additional optics are inserted in the lightpath.

## 2.6 Phase Shifting Holography [7,9]

### 2.6.1 Method A

When a phase  $\alpha$  is added to the reference beam by means of a piezoelectric transducer (PZT) for example, Equations 1-3 remain valid provided that the additional phase is inserted in the cosine of (3). The intensity distribution in the CCD plane is given by (21):

$$I_{\alpha}(x_2, y_2) = R_0^2 + |o(x_2, y_2)|^2 + 2R_0|o(x_2, y_2)|\cos(\theta_c(x_2, y_2) + \alpha) \quad (21)$$

The intensity difference  $\Delta I(x_2, y_2)$  to be considered here is the difference between the recorded interference pattern  $I(x_2, y_2)$  without phase shift as in (3) and the recorded interference pattern  $I_{\alpha}(x_2, y_2)$  with phase shift  $\alpha$ . The term  $\cos(\theta_c(x_2, y_2) + \alpha)$  that appears from (21) is developed using conventional trigonometric relations, and the resulting expression of  $\Delta I_{\alpha}(x_2, y_2)$  is rewritten with complex exponentials. The calculations here are very similar to the ones developed for the HRO method and the expression obtained for  $\Delta I(x_2, y_2)$  is the same as the one of (17), provided that  $J(x_2, y_2)$  is replaced by  $(1 - \exp(i\alpha))J(x_2, y_2)$ .

Consequently, the reconstructed hologram  $U(p, q)$  may be described by (22):

$$U(p, q) = R_0[(1 - \exp(i\alpha))V(p, q) + (1 - \exp(-i\alpha))V^*(-p, -q)] \quad (22)$$

Since the distribution  $U(p, q)$  is similar to the one obtained with the HRO method, the same conclusions apply: the zero order is unexistent and the nonoverlapping condition for the higher orders is the same. What differs here is the presence of the factor  $1 - \exp(i\alpha)$  that controls the strength of the reconstructed object regarding the noise floor, the latter being fixed by the condition  $\alpha = 0$ . This implies that  $\Delta I(x_2, y_2)$  is exactly equal to 0 in theory. On the other extreme, the maximum amplitude for the reconstructed object is reached for a phase shift of  $\alpha = \pm\pi$ , which gives an optimal contrast. However, we believe that adjusting a same phase shift for every

pixel in the image is a difficult task as all the light paths are not parallel or can be disturbed by conditions that are fluctuating. It is worth mentioning that  $U(p, q)$  will exhibit the reconstructed object without the zero-order image as soon as  $\alpha$  departs from 0. For that reason, we believe that subtraction digital holography is a special case of phase shifting subtraction holography with an uncontrolled phase shift  $\alpha$ . The zero-order image is eliminated if  $\alpha = \pm\pi$ , and the conjugate image is eliminated if  $\alpha = \pi/2$ .

The difference between the methods that have been exposed in this paper is that while subtraction digital holography may work in a hostile environment, HRO and subtraction phase shifting holography require rigorously controlled conditions to give optimal results.

### 2.6.2 Method B

This method requires the capture of three images with different phase modulations,  $\theta$ ,  $\theta_1$  and  $\theta_2$  between the reference beam and the object beam. The intensity distributions corresponding to each phase shift can be described by the following equations (23-24):

$$I_{\alpha}(\theta_1) = R^2 + |O(x_2, y_2)|^2 + 2R|O(x_2, y_2)|\cos\{\theta_c(x_2, y_2) + \theta_1\} \\ = R^2 + |O(x_2, y_2)|^2 + R^*O(x_2, y_2)e^{i(\theta_c + \theta_1)} + RO^*(x_2, y_2)e^{-i(\theta_c + \theta_1)} \quad (23)$$

$$I_{\alpha}(\theta_2) = R^2 + |O(x_2, y_2)|^2 + 2R|O(x_2, y_2)|\cos\{\theta_c(x_2, y_2) + \theta_2\} \\ = R^2 + |O(x_2, y_2)|^2 + R^*O(x_2, y_2)e^{i(\theta_c + \theta_2)} + RO^*(x_2, y_2)e^{-i(\theta_c + \theta_2)} \quad (24)$$

These two intensity distributions and the intensity distribution with zero phase modulation  $I$  are used to obtain the  $OR^*$  term as shown in (25):

$$\exp(i\theta_1)I_{\alpha}(\theta_1) - \exp(i\theta_2)I_{\alpha}(\theta_2) + [\exp(i\theta_1) + \exp(-i\theta_2)]I \\ = \left\{ \frac{[e^{i(\theta_c + \theta_1)} - 1]}{[e^{-i(\theta_c + \theta_1)} - 1]} - \frac{[e^{i(\theta_c + \theta_2)} - 1]}{[e^{-i(\theta_c + \theta_2)} - 1]} \right\} OR^* \quad (25)$$

For  $\theta_1 = 2\pi/3$  and  $\theta_2 = -2\pi/3$ , it can be verified that the zero order and the twin image are eliminated.

## 2.7 Mean Value Subtraction [5]

The bright central spot appearing in most digital reconstructions is the undiffracted reconstruction wave. This zero order or DC term disturbs the image, because it may partially or totally cover the reconstructed object. As for the elimination of the zero-order disturbance, Kreis and Jüptner[5] proposed a purely numerical method

which consists of subtracting the average intensity from each stored hologram.

The average intensity of all pixels within the image is given by (26):

$$H_m = \frac{1}{NM} \sum_{k=0}^{N-1} \sum_{l=0}^{M-1} H(k\Delta x, l\Delta y) \quad (26)$$

where  $H(k\Delta\xi, l\Delta\eta)$  designates the hologram.

The zero order can be suppressed by subtracting this average intensity  $H_m$  from each pixel such as in (27):

$$H'(k\Delta x, l\Delta y) = H(k\Delta x, l\Delta y) - H_m \quad (27)$$

The reconstruction of  $H'$  would provide an image free of the zero-order. While  $H$  has only positive values,  $H'$  may exhibit negative intensities as it is downshifted by performing (27).

### 2.8 Digital Lowpass Filter: Method C [6,16]

This method uses a low-pass filter to select the region of interest on the power spectrum of the reconstructed hologram. Once the size and the position of the filtering window have been estimated, the twin image will be removed by spatial filtering in the Fourier space, while the zero order is eliminated by applying the method of mean value subtraction. The mathematical description is provided in Equation (28):

$$O(x_2, y_2) = R^* \cdot \text{FT}^{-1} \left\{ \text{FT} \left[ H'(x_2, y_2) \exp \left[ i \frac{\pi}{\lambda d'} (x_2^2 + y_2^2) \right] \right] \cdot [\text{spatial filter}] \right\} \quad (28)$$

with  $H'(x_2, y_2) = H(x_2, y_2) - H_m$

and:

$$H_m = \frac{1}{NM} \sum_{k=0}^{N-1} \sum_{l=0}^{M-1} H(k\Delta x, l\Delta y).$$

Only a single image is needed for this method of removing unwanted components.

## 3. EXPERIMENTS

### 3.1 Quasi-Fourier Off-axis Configuration

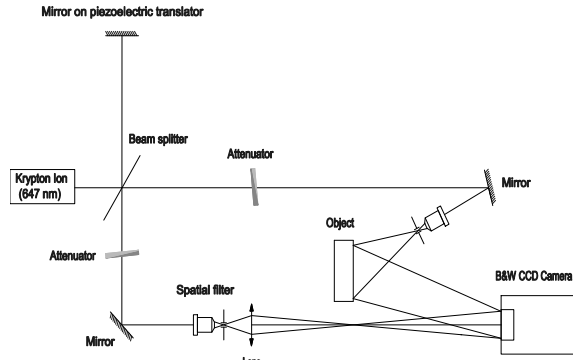


Figure 4: Recording Setup (Quasi-Fourier Off-axis Configuration).

In order to illustrate the theoretical investigations that have been conducted, a set-up has been built. It is sketched Fig. 4. A Krypton-Ion laser ( $\lambda = 647\text{nm}$ ) has been used as a light source. Its beam is split into an object beam and a reference beam. The object beam is expanded and directed onto a vibrating membrane that serves as the object. The reference beam can be modulated by a mirror mounted on a piezoelectric transducer (PZT), spatially filtered and focused off-axis in the plane of the object. This is the reference point-source required for off-axis Fourier recordings. With the PZT, the phase of the reference wave can be shifted. The intensity ratio between the reference beam and the object beam is adjusted to 3:1 with a set of neutral density filters. Holograms are recorded at about 1 meter away from the object with the CCD sensor of a Lumenera Infinity 2 digital camera (Sony ICX205AK monochrome sensor,  $1392 \times 1040$  square pixels with  $4.65\mu\text{m}$  pitch, 8 bits).



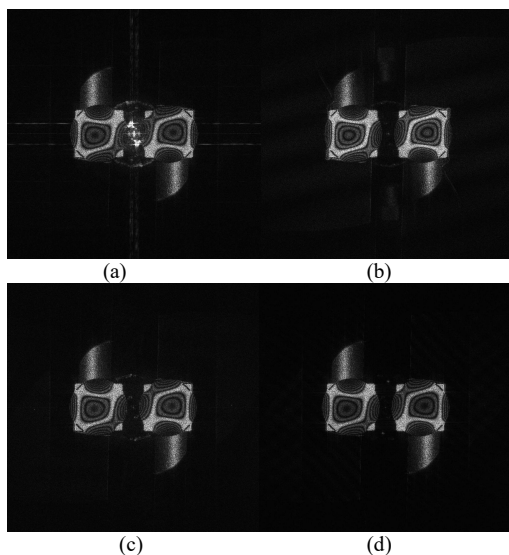


Figure 5: Reconstruction With Digital Interferograms: a) DFT Of An Interferogram, b) Subtraction Digital Holography, c) HRO Subtraction Method, d) Phase Shifting Subtraction Holography.

The images resulting from the methods reviewed in this paper are given in Fig. 5. The object under study, the membrane, is forced to vibrate mechanically. The interferograms are captured while it is vibrating and reconstruction is achieved according to the procedures reviewed in this paper. It is interesting to note that all the images exhibit the same vibration modes of the membrane, which validates the physical content of the reconstructed images. Image 5a gives an idea of the disturbance that might affect the DFT of a single interferogram; there are sharp peaks at the center, some horizontal and vertical lines that might be caused by the sampling mesh. As to the zero-order elimination, it appears that all the methods have almost the same performance, at least visually.

This means that the very basic approach of subtraction digital holography (Image 5b) is capable of providing the same quality of image reconstruction as the HRO method (Image 5c) which requires tight constraints on stability, and as the phase shifting holography (Image 5d) which is experimentally more sophisticated. For that reason, we believe that subtraction digital holography which does not require any heavy equipment, can be very effective for applications like quality control or structure deformation.

### 3.2 Fresnel configuration

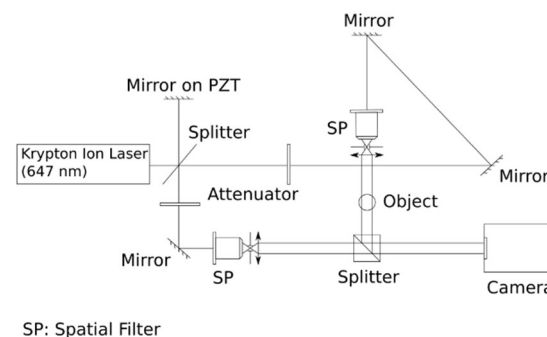


Figure 6: Recording Set-up (Fresnel Configuration).

For such a configuration, the object and its illumination settings have been modified. This means that the whole block on the right hand side of Fig. 4 has been redesigned as a beam splitter is introduced. The modified set-up is sketched in Fig. 6. The expanded and collimated object beam now illuminates a stick-shaped diffuser. The reference beam is also expanded and collimated, while the intensity ratio between the reference beam and the object beam is kept to 3:1. Holograms are recorded at about 91 centimeters away from the object with the same camera as for the off-axis Fourier holography. Applying the methods reviewed in this paper provides the results of Figures 7-10.

As for A and B, the results are provided in Figures 7(b) and 7(c) where the reduction or elimination of the zero-order image can be observed. It is worth mentioning that the reconstructions obtained from these methods appear to be less noisy.

For illustration purpose, the effects of mean subtraction may be assessed in Figures 8(a) and (b): it can be seen that the bright spot at the center has been significantly reduced in Figure 8(b).

We have also compared HRO to  $A(\alpha=\pi/2)$  and B. The results are shown in Figure 9. As for the zero order and the conjugate image elimination, minimal noise has been achieved with method B.

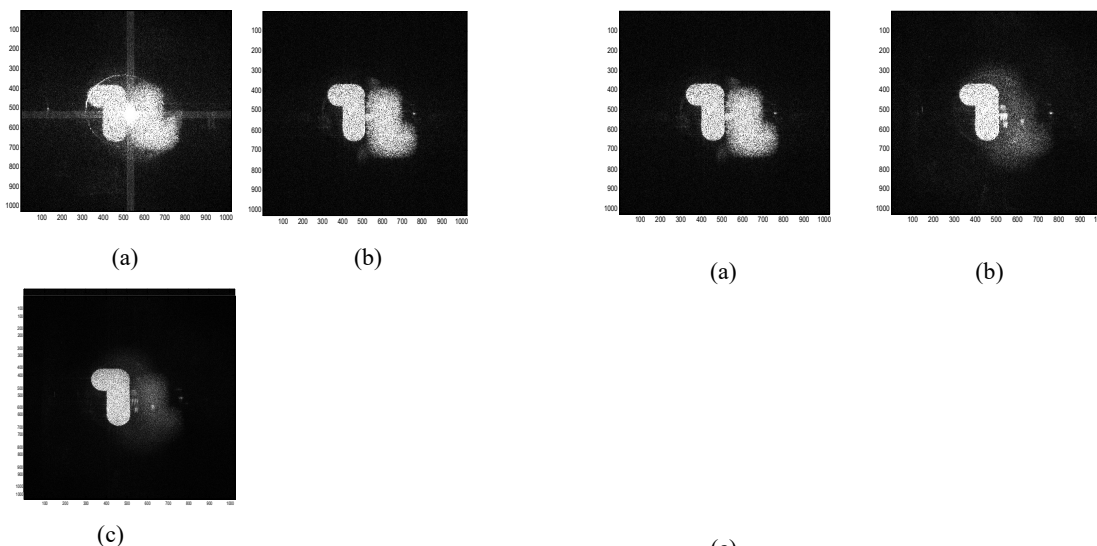


Figure 7: Zero-order Elimination. Reconstruction a) of the Recorded Hologram, b) with the HRO Method and c) Phase Shifting Holography.

Figure 9: Zero Order and Conjugate Image Elimination. Reconstruction Using (a) HRO, (b) Method A and (c) Method B. The Latter Appears to be the Most Efficient Here.

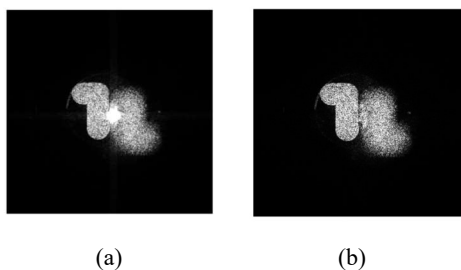


Figure 8: Zero-order Elimination. Reconstruction a) of the Raw Hologram and (b) Using the Mean Value Subtraction Method.

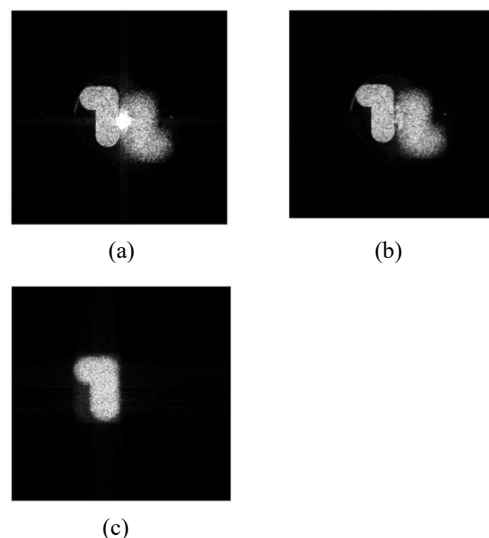


Figure 10: Zero Order and Conjugate Image Elimination. Reconstruction with (a) the Recorded Hologram, (b) Using Mean Value Subtraction, and (c) Method C.

The case of zero order and twin image elimination for a single recording is shown in Figure 10 where (b) and (c) are reconstructions without and with spatial filtering, after subtracting the hologram mean value. In Figure 10(c), a rectangle window of size  $200 \times 188$  has been used. The performance of method C indicates it may be used for real time reconstruction as it requires only one captured digital hologram and the operations required for removing the zero order and twin image are fast. As frequency filtering is involved, it should be mentioned that bandwidth reduction is inevitable.

#### 4. CONCLUSION

Methods for eliminating the zero order and the conjugate image in digital holography have been investigated. The advantage of the subtraction digital holography approach is that it is easy to achieve. It consists of subtracting two holograms recorded at different times. The method is efficient for off-axis

Fourier holograms as the interference patterns differ from each other by an amount of phase shift, and which would not vary too much during the recording procedure. This is the case when low intensity slow perturbations are present. The drawback is that as the shifts are random, it is difficult to determine when the result may be acceptable. On the other hand, HRO and phase shifting are deterministic procedures that are very effective for eliminating the zero order and the conjugate image. They may be used for both quasi-Fourier off-axis and Fresnel holograms. The drawback is that both require the capture of multiple images in the same recording conditions or to insert additional optics in the pathway of the wavefront. For that reason, they should be used in a highly stable environment. As of the purely digital technique exposed here, it only requires the capture of a single hologram and the operations involved in the filtering procedure are fast. The drawback is that the image bandwidth and consequently, the resolution is reduced.

To illustrate the theoretical investigations, both off-axis Fourier and Fresnel configurations have been experimented. The sample was a vibrating membrane in the first case so that reflection holography is considered, while a stick-shaped transmission diffuser has been selected for the second case. As for off-axis Fourier holography, HRO and deterministic phase shifting methods provide high quality results for zero-order elimination, while subtraction digital holography requires an operator for selecting the best frame amongst the two-by-two subtracted holograms. In the case of Fresnel digital holography, HRO and phase shifting are less efficient. However, a pure and basic digital technique that combines mean value subtraction and spatial filtering in the Fourier space has rendered reconstructions that are more than acceptable in the context of both zero order and twin image elimination using a single hologram. The cost is that some blurring is introduced as a result of bandwidth reduction.

#### REFERENCES:

- [1] J. W. Goodman, "Introduction à l'Optique de Fourier et à l'Holographie", 1st ed. Masson, 1972.
- [2] D. Gabor, "A New Microscopic Principle", *Nature*, Vol.161, 1948, pp.777- 778.
- [3] E. N. Leith, and J. Upatnieks, "Reconstructed Wavefronts and Communication Theory", *Journal of the Optical Society of America*, Vol. 52, No. 10, 1962, pp. 1123-1128.
- [4] Th. Kreis, "Handbook of Holographic Interferometry: Optical and Digital Methods", 1st ed., Wiley-VCH, Berlin, 2005, pp.105-106.
- [5] Th. Kreis, and W. Jüptner, "Suppression of the DC Term in Digital Holography", *Optical Engineering*, Vol. 36, No. 8, 1997, pp. 2357-2360.
- [6] T.-C. Poon, K. B. Doh, B. W. Schilling, M. H. Wu, K. Shinoda, and Y. Suzuki, "Three-dimensional Microscopy by Optical Scanning Holography", *Optical Engineering*, Vol. 34, No.5, 1995, pp. 1338-1344.
- [7] Y. Takaki, H. Kawai and H. Ohzu, "Hybrid Holographic Microscopy Free of Conjugate and Zero-Order Images", *Applied Optics*, Vol. 38, No. 23, 1999, pp. 4990-4996.
- [8] M.L. Rodriguez, J.A. Rayas, R.R. Cordero, A.M. Garcia, A.M. Gonzalez, A. T. Quiñones, P.Y. Contreras, and O.M. Cázares, "Dual plane slightly off-axis digital holography based on a single cube beam splitter", *Applied Optics*, Vol. 57, No. 10, 2018, pp. 2727-2735.
- [9] I. Yamaguchi, and T. Zhang, "Phase-shifting Digital Holography", *Optics Letters*, Vol. 22, No.16, 1997, pp. 1268-1270.
- [10] N. Yoshikawa, S. Namiki, and Atsushi Uoya, "Object wave retrieval using normalized holograms in three-step generalized phase-shifting digital holography", *Applied Optics*, Vol. 58, No.5, 2019, pp. A161-A168.
- [11] N. Demoli, J. Mestrovic, and I. Sovic, "Subtraction Digital Holography", *Applied Optics*, Vol. 42, 2003, pp. 798-804.
- [12] L. Onural, and P. D. Scott, "Digital Decoding of In-line Holograms", *Optical Engineering*, Vol. 26, No.23, 1987, pp.1124-1132.
- [13] L. Onural, and M. T. Özgen, "Extraction of Three-dimensional Object-location Information Directly from In-line Holograms using Wigner Analysis", *Journal of the Optical Society of America*, Vol. 9, No.2, 1992, pp. 252-260.
- [14] G. Pedrini, P. Fröning, H. Fessler, and H. J. Tiziani, "In-line Digital Holographic Interferometry", *Applied Optics*, Vol.37, No.26, 1998, pp.6262-6269.
- [15] G.-L. Chen, C.-Y. Lin, M.-K. Kuo, and C.-C. Chang, "Numerical Suppression of Zero order Image in Digital Holography," *Optics Express*, Vol.15, No.14, 2007, pp.8851-8856.
- [16] G.-L. Chen, C.-Y. Lin, M.-K. Kuo, and C.-C. Chang, "Numerical Reconstruction and Twin-image Suppression using an Off-axis Fresnel

- Digital Hologram”, Applied Physics B, Vol. 90, 2008, pp.527-532.
- [17] N. Pavillon, C. S. Seelamantula, J. Kühn, M. Unser, and C. Depeursinge, “Suppression of the zero-order term in off-axis digital holography through nonlinear filtering”, Applied Optics, Vol.48, No.34, 2009, pp. H186- H195, 2009.
- [18] N. Pavillon, C. Arfire, I. Bergoënd, and C. Depeursinge, “Iterative method for zero-order suppression in off-axis digital holography”, Optics Express, Vol.18, No.15, 2010, pp.15318-15331.
- [19] Z. Ma, L. Deng, Y. Yang, H. Zhai, and Q. Ge, “Numerical iterative approach for zero-order term elimination in off-axis digital holography,” Optics Express, Vol. 21, pp. 28314-28324, 2013.
- [20] Z. Dong, H. Wang, and X. Wang, “Automatic filtering for zero-order and twin-image elimination in off-axis digital holography”, Optical Engineering, Vol. 58, 2019, 023112.
- [21] H. Wang, M. Lyu, and G. Situ, “eHoloNet: a learning-based end-to end approach for in-line digital holographic reconstruction”, Optics Express, Vol. 26, No.18, 2018, pp. 22603-22614.
- [22] Z. Li, L. Li, Y. Qin, G. Li, D. Wang, and X. Zhou, “Resolution and quality enhancement in terahertz in-line holography by sub-pixel sampling with double-distance reconstruction”, Optics Express, Vol. 24, No.18, 2016, pp. 21134-21146, 2016.
- [23] R. N. Bracewell, “The Fourier Transform and Its Applications”, 3rd ed, McGraw-Hill, 2002.
- [24] R. C. Gonzalez, and R. E. Woods, “Digital Image Processing”, 2nd edition Addison-Wesley, 1993.